Northridge earthquake, are also expected, with an average repeat time of 40 to 52 years. The historic record of M 6.5 to 6.7 events in the Los Angeles Basin is still under the long-term predicted rate, even allowing for occasional large events.

Uncertainty in our results stems from three primary factors: the overall slip rate for the region, the maximum rupture size, and the effective fractal dimension implied by our choice of *b*-value and scaling coefficient in Eq. 2. (We do not consider the prima facie assumption of a fractal distribution to be at issue.) The first source of uncertainty is accounted for directly: Our results correspond to the range of slip rates determined from geologic and geodetic compilations (*1*, *2*). The second factor is also addressed: Maximum rupture lengths shorter than 100 km are discounted because of the unrealistically frequent rate of moderate events that is implied. We do not consider the third factor to be significant because of the nature of fractal distributions and earthquake scaling relations: A scaling constant of 1 instead of 0.86 (that is, a strictly self-similar distribution of rupture areas) in Eq. 2 would change Eq. 6 to $M_{o,total} = 1.45M_{o,1}$. This change would increase T_m by about 9% and increase the number of moderate events (M_w 6.6) from about six to nine.

Our calculations are independent of the known details of faulting and slip rates on individual faults in the region, as summarized by Dolan *et al.* (*1*). Their results can be compared to ours: The six multiple–fault-segment scenarios yield events with M_w 7.20 to 7.58, produced, on average, every 140 years. This value is about half of our preferred estimate but is not inconsistent with our results because 70 to 80% of the geologically determined scenario earthquakes have M_w = 7.2 to 7.3 (*14*). Also, the fractal analysis permits a fraction of the moment rate, approximately 30%, to be accounted for by moderate events.

REFERENCES AND NOTES

1. J. Dolan *et al.*, *Science* **267**, 199 (1995).
2. E. Hauksson, in *Engineering Geology Practice in Southern California*, B. Pipkin and R. Proctor, Eds. (Engineering Geologists Spec. Publ. 4, Star, Belmont, CA, 1993), pp. 167–179; K. Feigl *et al.*, *J. Geophys. Res.* **98**, 21677 (1993); A. Donellan *et al.*, *Nature* **366**, 333 (1993).
3. D. Jackson, *Seismol. Res. Lett.* **65**, A5 (abstr.) (1994).
4. K. Sieh *et al.*, *Science* **260**, 171 (1993).
5. Scientists of the U.S. Geological Survey and the Southern California Earthquake Center, *Science* **266**, 389 (1994).
6. P. G. Okubo and K. Aki, *J. Geophys. Res.* **92**, 345 (1987); C. J. Aviles, J. Boatwright, C. H. Scholz, *ibid.*, p. 331.
7. H. Kanamori and D. Anderson, *Bull. Seismol. Soc. Am.* **65**, 1073 (1975); D. Turcotte, *Pure Appl. Geophys.* **131**, 171 (1989).
8. S. Wesnousky *et al.*, *J. Geophys. Res.* **88**, 9331 (1983).
9. S. N. Ward, *Seismol. Res. Lett.* **65**, 63 (abstr.) (1994); D. D. Jackson *et al.*, *Eos* **74** (spring suppl.), 426 (1994).
10. T. Hanks and H. Kanamori, *J. Geophys. Res.* **84**, 2348 (1979).
11. Given Eq. 1 and the empirical scaling relation $d = \gamma L$ for a rectangular fault (*13*), M_o is expected to scale as WL^2. For crustal earthquakes, *W* will be bounded by the width of the brittle seismogenic zone; for large earthquakes, M_o is thus expected to scale as L^2.
12. Our calculations are for a seismogenic depth of 17.5 km; if we allow for dipping faults with greater down-dip width, one could obtain the same area and moment with a shorter fault (*1*).
13. C. H. Scholz et *al*, *Bull. Seismol. Soc. Am.* **76**, 68 (1986).
14. With the use of Eq. 3, a difference of 0.2 in M_w (between 7.25 and 7.45) implies a difference in seismic moment of a factor of 2. From Eq. 1, the implied difference in area is 1.7. A difference of 0.2 in M_w is thus nontrivial, and the shorter repeat time of these events dominates the average in the calculations by Dolan *et al.* (*1*) (the 70 to 80% range reflects the uncertainty in whether the Santa Monica mountains system will rupture as a whole or in subsystems).

15. I thank S. Ward, J. Vidale, S. Wesnousky, and an anonymous reviewer for their constructive reviews. I especially thank J. Dolan and K. Sieh for many helpful discussions.

26 August 1994; accepted 9 November 1994

Rapid Accretion and Early Differentiation of Mars Indicated by ^{142}Nd/^{144}Nd in SNC Meteorites

Charles L. Harper Jr.,* Laurence E. Nyquist, Brij Bansal, Henry Wiesmann, Chi-Yu Shih

Small differences in the ratio of neodymium-142 to neodymium-144 in early formed mantle reservoirs in planetary bodies are the result of in situ decay of the extinct radionuclide samarium-146 and can be used to constrain early planetary differentiation and therefore the time scale of planetary accretion. The martian meteorite Nakhla (~1.3 billion years old), the type sample of the nakhlite subgroup of the Shergottite-Nakhlite-Chassigny (SNC) meteorites, exhibits a 59 ± 13 parts per million excess in the ratio of neodymium-142 to neodymium-144 relative to normal neodymium. This anomaly records differentiation in the martian mantle before 4539 million years ago and implies that Mars experienced no giant impacts at any time later than 27 million years after the origin of the solar system.

Planets in the inner solar system are widely believed to have accreted from an initial swarm of planetesimals by hierarchical coagulation, which involves the merging of objects of increasing size until only a small number of large objects remain in each radial zone (*1*). According to this view, the late stages of planetary accretion are dominated by a few giant impacts. The spins of both Earth and Mars are consistent with one or more of these events during accretion (*2*). Giant impacts generate transient, mantle-wide magma oceans, and therefore the histories of the terrestrial planets are expected to have begun with an epoch of giant impacts and magma oceans. However, the durations for these accretionary epochs are unknown. Estimates from planetesimal coagulation models are generically uncertain at late times and fundamental issues remain unresolved, so isotopic age determinations are needed to constrain accretion and giant impact time scales directly.

The presence of a small but significant abundance of ^{146}Sm (which decays by α emission to ^{142}Nd with a half-life of 103 million years) in the early solar system provides a means for dating early episodes of differentiation in planetary bodies based on the preservation of isotopic signatures at depth in mantle reservoirs (*3*). The ^{146}Sm-^{142}Nd system is ideal for dating differentiation episodes in the silicate portions of planets because other large-scale cosmochemical processes such as volatile depletion or core formation do not fractionate Sm/Nd and because this system can be linked to the long-lived ^{147}Sm-^{143}Nd system. Because the initial solar system abundance of ^{146}Sm was small [^{146}Sm/^{144}Sm = 0.0080 ± 0.0010 at 4566 million years ago (Ma) (*4*)] and the range of Sm/Nd fractionation in large-scale reservoirs is limited, ^{142}Nd/^{144}Nd shifts resulting from ^{146}Sm decay are generally expected to be less than one part in 10^4 (= 1 ϵ-unit). Use of the ^{146}Sm-^{142}Nd systematics therefore requires accurate determination of ^{142}Nd/^{144}Nd shifts at a resolution of better than 20 ppm (±0.2 ϵ-unit) relative to a reference standard. We report well-resolved ^{142}Nd shifts in SNC meteorites and outline their significance for the early history of Mars (*5*), which is where these meteorites are thought to have been derived (*6*).

Identification of a ^{142}Nd anomaly in a

C. L. Harper Jr., Department of Earth and Planetary Sciences, Harvard University, 20 Oxford Street, Cambridge, MA 02138, USA.
L. E. Nyquist, National Aeronautics and Space Administration Johnson Space Center, Houston, TX 77058, USA.
B. Bansal, H. Wiesmann, C.-Y. Shih, Lockheed Engineering and Science Company, C23, 2400 NASA Road 1, Houston, TX 77058, USA.

*To whom correspondence should be addressed.

mantle source region implies that silicate reservoirs fractionated in the first few hundred million years of solar system history because the ^{146}Sm chronometer becomes effectively extinct after two or three half-lives, or about 300 million years. Information on the early formation history of any reservoir is retained in the ^{142}Nd/^{144}Nd ratio of a reservoir and is carried by any sample derived from it by melt extraction.

In its simplest formulation, a ^{142}Nd/^{144}Nd anomaly can be modeled as the result of a single fractionation of an unfractionated precursor reservoir. In this case ^{146}Sm decay generates only ^{142}Nd shifts (deviations with respect to ^{142}Nd/^{144}Nd in an unfractionated reservoir) after separation and before ~300 million years. The age (t_2) of the fractionation is obtained from

$$(\epsilon^{142\text{Nd}})_t = Q_{142} f_i^{\text{Sm/Nd}} (^{146}\text{Sm}/^{144}\text{Sm})_{t_1} e^{-\Delta t_i/\tau_{146}} \quad (1)$$

where $\Delta t_i = (t_1 - t_2)$, $Q_{142} = 354$, $(^{146}\text{Sm}/^{144}\text{Sm})_{t_1}$ is the ab initio solar system ^{146}Sm isotopic abundance at t_1 = 4566 Ma, $f_i^{\text{Sm/Nd}}$ is the Sm/Nd fractionation factor, and τ_{146} is the ^{146}Sm lifetime (149 million years) (7). The observable quantity $\epsilon_{^{142}\text{Nd}}$ is defined as the post-decay or present-day deviation from the composition of an Sm/Nd-unfractionated chondritic uniform reservoir (CHUR) (7). Values of $f_i^{\text{Sm/Nd}}$ may be obtained from the long-lived ^{147}Sm-^{143}Nd system. In Eq. 1 it is assumed that ^{146}Sm has decayed before any further fractionation events.

We studied all known SNC meteorites with the exception of the two most recently identified Antarctic specimens (LEW 88516 and ALHA 84001). Determinations of source ages require accurate estimates of Sm/Nd at early times when ^{146}Sm was decaying. The rare-earth elements in the SNC meteorites were strongly fractionated during melt extraction from source regions, and back-projections based on partitioning models are highly uncertain. The NC meteorites (nakhlites and Chassigny) are thought to represent cooled magma extracted from the martian mantle ~1.3 billion

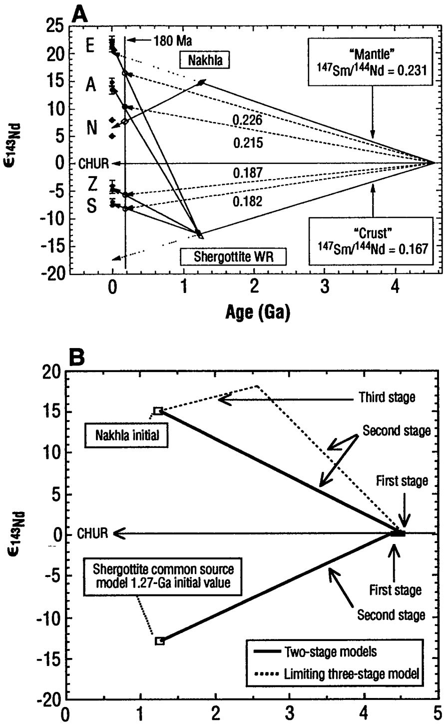

Fig. 1. (**A**) An $\epsilon_{^{143}\text{Nd}}$ time evolution plot for SNC meteorites and their source reservoirs showing growth in parts-in-10^4 deviation (ϵ-units) in ^{143}Nd/^{144}Nd relative to that of CHUR. A single stage of evolution for the Nakhla source (N) is shown by the uppermost solid line (labeled "mantle") connecting the Nakhla initial point to the horizontal CHUR line at 4.57 Ga. In the case of the shergottites, estimation of ^{147}Sm/^{144}Nd in source reservoirs is problematic because of the complex isotopic record in these meteorites. A "common source" interpretation (unbroken lines) is based on the apparent isochronous relation for the whole-rock (WR) shergottites, shown by the convergence of their evolution paths for Shergotty (S), Zagami (Z), ALHA 77005 (A), and EETA 79001 (E) at 1.3 billion years. An alternate "multiple source" interpretation (broken lines) follows evidence for an ~180-Ma crystallization age for the shergottites. A range of initial $\epsilon_{^{143}\text{Nd}}$ values is given by intersections of WR evolution paths with the vertical line at 180 Ma. Single-stage evolution paths for these sources are drawn for the interval 180 Ma to 4.57 Ga. (Marked values are ^{147}Sm/^{144}Nd ratios.) (**B**) Schematic of possible reservoir formation and evolution histories subject to constraints from ^{142}Nd/^{144}Nd. Two possible evolution paths for two- and three-stage models of the Nakhla source are shown in the positive $\epsilon_{^{143}\text{Nd}}$ field. The (limiting) three-stage model has been selected to have a second-stage fractionation factor of 2 times that of the two-stage model.

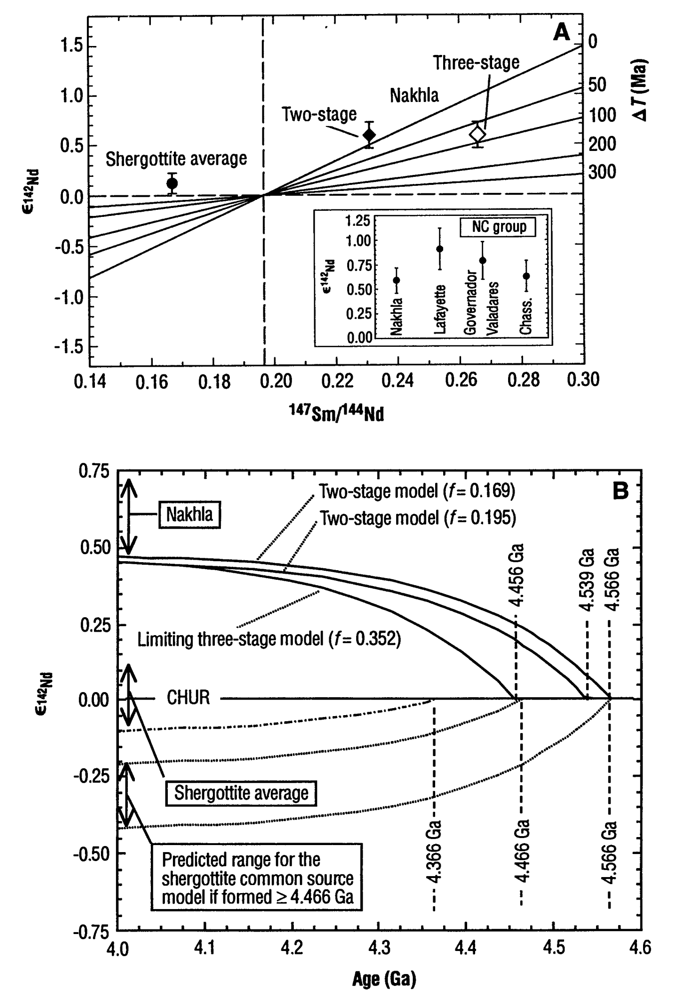

Fig. 2. (**A**) An $\epsilon_{^{142}\text{Nd}}$ isochron plot for the Nakhla source and the shergottite common source model. Individual data for the NC group meteorites are shown in the inset. The model age range for formation of the Nakhla source is obtained from tie lines connecting the data range to the CHUR reference point (^{147}Sm/^{144}Nd = 0.1967; $\epsilon_{^{142}\text{Nd}}$ = 0) and can be read off the ΔT scale. The (preferred) two-stage model is for a single stage of fractionation with ^{147}Sm/^{144}Nd = 0.230 ($f^{\text{Sm/Nd}}$ = 0.169) obtained from a self-consistent two-stage model of $\epsilon_{^{143}\text{Nd}}$ evolution, as shown in the upper part of Fig. 1B (solid line). The limiting three-stage model is for the more complicated (extreme) model of $\epsilon_{^{143}\text{Nd}}$ evolution (^{147}Sm/^{144}Nd = 0.266; $f^{\text{Sm/Nd}}$ = 0.352) shown by dashed lines in the upper part of Fig. 1B. (**B**) Time evolution plot for $\epsilon_{^{143}\text{Nd}}$ with fractionated mantle reservoirs indicated by curved evolution paths diverging from CHUR at their time of formation. The lowest age possible for differentiation of the Nakhla source is 4.539 Ga in the preferred two-stage model ($f^{\text{Sm/Nd}} \leq 0.195$). In the extreme case of the three-stage model ($f^{\text{Sm/Nd}} \leq 0.352$, see Fig. 1B), a source formation age as low as 4.456 Ga is allowed. Evolution paths for a source with $f_i^{\text{Sm/Nd}} = -0.151$ are shown as dashed curves in the lower half of (B) for formation times of ΔT = 0 and 100 Ma, and as a dot-dash curve for ΔT = 200 Ma. If the shergottites were derived from a common source 1.3 Ga ago (Fig. 1A, solid lines), then this source must have been derived from a domain that either involved planetary recycling or remained unfractionated in the martian mantle for at least the first 200 million years of solar system history (dot-dash curve). It cannot have formed contemporaneously with the Nakhla source with Sm/Nd as fractionated as $f_i^{\text{Sm/Nd}} = -0.151$.

years ago (Ga). The initial $\epsilon_{^{143}Nd}$ of $\sim+15 \pm 1$ ϵ-units in Nakhla (*8*) at the time of melt extraction at ~1.3 Ga (*9*) identifies the Nakhla source as an ancient depleted mantle reservoir with time-integrated $^{147}Sm/^{144}Nd \geq 0.230$ ($f^{Sm/Nd} \geq 0.169$), as shown in Fig. 1. Such ^{147}Sm-^{143}Nd studies have not been carried out on the other nakhlites and Chassigny. However, ages determined by the ^{87}Rb-^{87}Sr (*10*) and ^{39}Ar-^{40}Ar (*9, 11*) methods are in good agreement with the Nakhla age. All of the NC meteorites have overlapping cosmic-ray exposure ages and were likely ejected from a common source crater on Mars at ~10 Ma (*12*). For age determination of the Nakhla source reservoir, we use $^{147}Sm/^{144}Nd \geq 0.230$ ($f^{Sm/Nd} \geq 0.169$) as a lower limit, and $^{147}Sm/^{144}Nd \leq 0.266$($f^{Sm/Nd} \leq 0.352$) as a reasonable upper limit (Figs. 1 and 2). A shift in $\epsilon_{^{143}Nd}$ of +16 would take place in only 1.6 billion years at the latter level, or half the time available between the origin of the solar system and extraction of the melt parental to Nakhla at 1.3 Ga.

Constraints on Sm/Nd in the shergottite source reservoir or reservoirs are highly uncertain. Alternate and widely differing interpretations are shown in Fig. 1A.

The crux in the application of ^{146}Sm-^{142}Nd systematics to planetary studies is measurements of the $^{142}Nd/^{144}Nd$ ratio. Ninety-one standards and a large number of contemporaneous multiple sample runs obtained during this study indicate a single-run precision of ±29 ppm (2σ) if a $^{146}Nd/^{144}Nd$ normalization is used to correct for mass-dependent discrimination (1 ϵ-unit = 100 ppm). By running Nd samples multiple times, we found that it was possible to decrease this uncertainty. In some cases additional reduction was provided by the consideration of data alternately normalized to $^{148}Nd/^{144}Nd$. We examined $^{145}Nd/^{144}Nd$ measurements as a diagnostic for interferences on masses 144 and 146, which were not observed. Well-resolved shifts in $^{142}Nd/^{144}Nd$ with respect to our terrestrial standard are apparent in all four NC group meteorites (Table 1). The shift in Nakhla is 59 ± 13 (2σ) ppm higher than the standard. The average shift for the NC group is the same within error (+69 ± 8 ppm). The shergottites do not exhibit any $^{142}Nd/^{144}Nd$ difference from the standard at the >30-ppm level.

Table 1. Measured values of $^{142}Nd/^{144}Nd$ for SNC meteorites reported as deviations from the terrestrial standard composition in ϵ-units. All measurements were made by static multicollection on a seven-cup Finnigan MAT 261 mass spectrometer. *N* is the number of replicate runs for each sample; Norm. designates the normalization used in the measurement: $^{146}Nd/^{144}Nd$, $^{148}Nd/^{144}Nd$, or a combination of both data sets. When both normalizations were used, the one with the greater statistical weight is given first. The one with the lesser statistical weight is given in parentheses. Details of the measurement procedure are given in (*27*).

Sample	*N*	Norm. ($^{i}Nd/^{144}Nd$)	Mean (ϵ-units)
NC suite			
Nakhla	4	146(148)	0.59 ± 0.13
Lafayette	3	146	0.91 ± 0.21
Governador Valadares	3	146	0.79 ± 0.19
Chassigny	3	148(146)	0.63 ± 0.16
Average NC meteorites	13		0.69 ± 0.08
Shergottites			
Shergotty	3	146	0.28 ± 0.19
Zagami	4	146	−0.09 ± 0.18
ALHA77005	1	146	−0.17 ± 0.32
EETA79001A	2	146	0.26 ± 0.23
EETA79001B	1	146	0.30 ± 0.29
Average shergottites	11		0.12 ± 0.10

The data provide three first-order constraints on martian geochemical reservoirs. First, $\epsilon_{^{142}Nd}$ differences indicate derivation of the parent melts of the NC group and shergottite meteorites from distinct sources. Second, the data constrain assimilation-mixing relations as proposed in several petrologic models (*13, 14*). Several interpretations have proposed derivation of the shergottites at 180 Ma from NC source melts assimilating crust represented by an abundant component in the Shergotty and Zagami meteorites (*13, 14*). The measured $\epsilon_{^{142}Nd}$ values and projection of the whole-rock $\epsilon_{^{142}Nd}$ values to 180 Ma, however, are clearly inconsistent with two-component mixing (Fig. 3). Third, the data provide a test of the shergottite common source model, as shown in

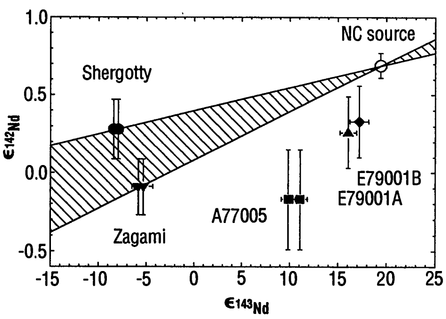

Fig. 3. Plot of $\epsilon_{^{142}Nd}$ data for the shergottite meteorites versus time-projected $\epsilon_{^{143}Nd}$ for these rocks when their parent melts crystallized at ~180 Ma. Mixing relations are linear in this plot. Mantle melts from the NC source assimilating a putative crustal component present in Shergotty and Zagami at 180 Ma are constrained to the cross-hatched area. Meteorites A77005 and E79001A and B do not plot within this zone and therefore are inconsistent with a two-component mixing model. The parental melts of the shergottites do not appear to have been derived from the NC source.

Fig. 1A. If the shergottites were derived from a common "enriched" [rich in light rare-earth elements (LREEs)] reservoir at 1.3 Ga (as implied by the solid-line evolution model in Fig. 1A), and if this reservoir formed contemporaneously as a differentiation complement to the "depleted" (LREE-poor) NC parent reservoir, then a resolvably negative $^{142}Nd/^{144}Nd$ anomaly of magnitude nearly equal to that of Nakhla should be present (Fig. 2B). The absence of resolvable shifts in the shergottites clearly rules out this version of the common-source reservoir model of the shergottites (Fig. 1A).

The mantle sources from which the shergottite meteorites were derived do not appear to have formed contemporaneously with the NC source with Sm/Nd fractionation as large as the value of $f^{Sm/Nd} = -0.151$ implied in the common source model (Fig. 1A). Three broad interpretations are possible: either (i) some parts of the martian mantle remained undifferentiated at early times, or the shergottites were derived either from (ii) remixed mantle or from (iii) remelted protocrust with $f^{Sm/Nd} \approx 0$. In terms of the first interpretation, a mantle region would need to have remained unfractionated for at least the first ~200 million years of solar system history before fractionation to form a reservoir with $f^{Sm/Nd} = -0.151$ (Fig. 2B). The second interpretation would require plate recycling of the protocrust back into the mantle, unless fractionation of the martian mantle was due to crystal fractionation in a lunar-type magma ocean differentiation series rather than extraction of partial melts to form crust. The third idea that the shergottite source or sources might be remelted protocrust with $f^{Sm/Nd} \approx 0$ is an intriguing one that follows Sleep's (*15*) interpretation of the great crustal dichotomy of Mars as a result of a martian variant of sea-floor spreading. The ~180-Ma crystallization ages of the shergottites limit the location of their source crater to be in a young volcanic terrain, most likely the Tharsis Montes volcanic-tectonic belt (*16*), which lies on the dichotomy boundary and is interpreted by Sleep as an island arc. It may be possible to explain the considerable petrochemical complexity of the shergottites in the context of a convergent margin scenario.

The data also constrain the planetary accretion time scale of Mars. This is based on interpretation of the ^{146}Sm-^{142}Nd chronometer as recording differentiation only since the last episode of mantle rehomogenization associated with accretion. In the case of Mars, impact of an object with a mass one-tenth that of Mars is expected to generate a magma ocean ~500 km deep if the target material is at the solidus and if contributions from partial melting throughout the planet are included (*17*). Although it is not clear that partial melts will contribute to a magma ocean, convective velocities throughout the mantle clearly would increased by orders of magnitude in the presence of pervasive partial melting. For the purposes of this discussion, we assume that an impact of a ≥0.1 Mars mass object would isotopically remix the silicate portion of the merged object. In this case, the oldest age for silicate mantle differentiation yields a lower limit on the last event in the hierarchical accretion series.

The magnitude of $\epsilon_{^{142}Nd}$ in the NC group meteorites unambiguously confirms hints of very early martian mantle differentiation from the long-lived ^{87}Rb-^{87}Sr, ^{147}Sm-^{143}Nd, and ^{235,238}U-^{207,206}Pb systems (*18*). Because Nakhla is the only NC meteorite for which an initial $\epsilon_{^{142}Nd}$ value is known, determination of the age of mantle differentiation on Mars applies strictly only to its mantle source. On the basis of $\epsilon_{^{142}Nd} = 0.59 \pm 0.13$, we obtain a model age of 4.57 to 4.46 Ga for an initial fractionation range $0.230 \leq {}^{147}Sm/{}^{144}Nd \leq 0.266$ ($0.169 \leq f^{Sm/Nd} \leq 0.352$). This age is for a single differentiation episode. The lower age limit of 4.46 Ga corresponds to the time of formation of a reservoir with twice the single-stage $f^{Sm/Nd}$ required to generate $\epsilon_{^{142}Nd} = +16$ in the Nakhla source in 3.3 billion years.

The range for a two-stage model in the coupled ^{146,147}Sm-^{142,143}Nd systematics (*3*) is more tightly constrained (4566 million to 4539 million years), because the ^{147}Sm-^{143}Nd data limit fractionation in the source to $0.229 \leq {}^{147}Sm/{}^{144}Nd \leq 0.235$ ($0.165 \leq f^{Sm/Nd} \leq 0.195$). The two-stage model is more likely than the three-stage model because both systems are concordant within uncertainty for $t_2 = 4566$ Ma and $^{147}Sm/^{144}Nd = 0.235$ ($f_i^{Sm/Nd} = 0.195$). Thus, silicate mantle differentiation probably occurred within 27 million years of the formation of the solar system. Use of the NC group average $^{142}Nd/^{144}Nd$ shift ($\epsilon_{^{142}Nd} = 0.69 \pm 0.8$) would restrict this accretion interval even further.

This constraint may be useful in assessing the role of Jupiter in planetary accretion. It is widely believed that the existence of the asteroid belt rather than a planet in the region 2 to 4 astronomical units is the consequence of the rapid formation of proto-Jupiter on a 10^5- to 10^6-year time scale (*19*, *20*) during the time when planetary embryos were growing to the $\sim 10^{26}$-g scale in the region of the terrestrial planets (*21*). A related question is whether the small size of Mars (6×10^{26} g) is due to termination of the accretion process by jovian effects (*22*). Recent modeling suggests a time scale of <10 million years for gas accretion of Jupiter to attain its present mass (*23*). In the extreme case of removal of all objects in the Mars zone except for the largest "runaway embryo," Mars might be a fossil object from the pre-Jupiter coagulation epoch with an accretion time scale of <10 million years (*19*). The $\epsilon_{^{142}Nd}$ data are fully consistent with a rapid accretion time scale of this order. For comparison, a model planet in the vicinity of Mars was found to be ~70% accreted at 30 Ma in an average of six Monte Carlo coagulation simulations without jovian resonant influence (*24*). Because the simplest interpretation of the $\epsilon_{^{142}Nd}$ data is inconsistent with giant impacts ≥30 Ma (that is, later than 4536 Ma), the data hint that the accretion of Mars may have been truncated by the growth of Jupiter.

REFERENCES AND NOTES

1. G. W. Wetherill, *Annu. Rev. Earth Planet. Sci.* **18**, 205 (1990); J. J. Lissauer, *Annu. Rev. Astron. Astrophys.* **31**, 129 (1993).
2. J. J. Lissauer and V. S. Safronov, *Icarus* **93**, 288 (1991); L. Dones and S. Tremaine, *ibid.* **103**, 67 (1993).
3. C. L. Harper Jr. and S. B. Jacobsen, *Nature* **360**, 728 (1992); *Lunar Planet. Sci.* **XXV**, 509 (1994); L. E. Nyquist, H. Wiesmann, B. Bansal, C.-Y. Shih, *ibid.*, p. 1017.
4. L. E. Nyquist, B. Bansal, H. Wiesmann, C.-Y. Shih, *Meteoritics* **29**, 872 (1994); A. Prinzhofer, D. A. Papanastassiou, G. J. Wasserburg, *Geochim. Cosmochim. Acta* **56**, 797 (1992); G. W. Lugmair and S. J. G. Galer, *ibid.*, p. 1637; B. W. Stewart, D. A. Papanastassiou, G. J. Wasserburg, *ibid.* **58**, 3487 (1994).
5. L. E. Nyquist, C. L. Harper Jr., H. Wiesmann, B. Bansal, C.-Y. Shih, *Meteoritics* **26**, 381 (1991).
6. D. D. Bogard, L. E. Nyquist, P. Johnson, *Geochim. Cosmochim. Acta* **48**, 1723 (1984); H. Y. McSween Jr., *Rev. Geophys.* **23**, 391 (1985); *Meteoritics* **29**, 757 (1994); R. C. Wiens, R. H. Becker, R. O. Pepin, *Earth Planet. Sci. Lett.* **77**, 149 (1986); R. O. Pepin and M. H. Carr, in *Mars*, H. H. Keiffer and B. Jakosky, Eds. (Univ. of Arizona Press, Tucson, 1992), chap. 1.3, and references therein.
7. Additional definitions are as follows:

$$(\epsilon^{^{142}Nd})_i = \left[\frac{(^{142}Nd/^{144}Nd)_i}{(^{142}Nd/^{144}Nd)_{CHUR}} - 1\right] \times 10^4$$

and

$$f_i^{Sm/Nd} = \frac{(^{147}Sm/^{144}Nd)_i}{(^{147}Sm/^{144}Nd)_{CHUR}} - 1$$

where $(^{147}Sm/^{144}Nd)_{CHUR} = 0.1967$. We also assume:

$$(^{142}Nd/^{144}Nd)_{CHUR,\ present\ day} = (^{142}Nd/^{144}Nd)_{JSC/Ames}$$

where the subscript JSC/Ames refers to the composition determined for our Johnson Space Center (JSC) Ames metal standard. We find this standard to be isotopically indistinguishable from the California Institute of Technology Ndβ Ames metal standard. See S. B. Jacobsen and G. J. Wasserburg, *Earth Planet. Sci. Lett.* **67**, 137 (1984); *ibid.* **50**, 139 (1980); G. J. Wasserburg, S. B. Jacobsen, D. J. DePaolo, M. T. McCulloch, T. Wen, *Geochim. Cosmochim. Acta* **45**, 2311 (1981). For the age of the solar system, see C. Göpel, G. Manhes, and C. J. Allegre [*Earth Planet. Sci. Lett.* **121**, 153 (1994), and references therein]. Very high precision Nd isotope results obtained for the igneous meteorite Juvinas support this assumption to within ~0.1 ε-unit [C. L. Harper Jr. and S. B. Jacobsen, *Lunar Planet. Sci.* **XXIV**, 607 (1993); unpublished results].
8. N. Nakamura, D. M. Unruh, M. Tatsumoto, R. Hutchison, *Geochim. Cosmochim. Acta* **46**, 1555 (1982).
9. N. H. Gale, J. W. Arden, R. Hutchison, *Earth Planet. Sci. Lett.* **26**, 195 (1975); D. A. Papanastassiou and G. J. Wasserburg, *Geophys. Res. Lett.* **1**, 23 (1974); J. H. Chen and G. J. Wasserburg, *Lunar Planet. Sci.* **XVII**, 113 (1986); F. A. Podosek, *Earth Planet. Sci. Lett.* **19**, 135 (1973).
10. J. L. Wooden *et al.*, *Lunar Planet Sci.* **X**, 1379 (1979); N. Nakamura, H. Komi, H. Kagami, *Meteoritics* **17**, 257 (1982).
11. D. D. Bogard and L. Husain, *Geophys. Res. Lett.* **4**, 69 (1977); D. D. Bogard and L. E. Nyquist, *Meteoritics* **14**, 356 (1979).
12. D. D. Bogard, L. E. Nyquist, P. Johnson, *Geochim. Cosmochim. Acta* **48**, 1723 (1984); D. K. Pal *et al.*, *ibid.* **50**, 2405 (1986); U. Ott, *ibid.* **52**, 1937 (1988).
13. J. H. Jones, *ibid.* **50**, 969 (1986); J. H. Jones, *Proc. Lunar Planet. Sci. Conf.* **19**, 465 (1989); *Tech. Rep. 90-04* (Lunar and Planetary Institute, Houston, 1990), p. 35; J. Longhi, *Proc. Lunar Planet. Sci. Conf.* **21**, 695 (1991); M. D. Norman, *Lunar Planet. Sci.* **XXIII**, 999 (1992); E. Jagoutz, *Geochim. Cosmochim. Acta* **53**, 2429 (1989); M. Wadhwa, H. Y. McSween Jr., G. Crozaz, *Geochim. Cosmochim. Acta* **58**, 4213 (1994).
14. E. Jagoutz, *Space Sci. Rev.* **56**, 13 (1991).
15. N. H. Sleep, *J. Geophys. Res.* **99**, 5639 (1994).
16. P. J. Mouginis-Mark, T. J. McCoy, G. J. Taylor, K. Keil, *ibid.* **97**, 10213 (1992).
17. W. B. Tonks and H. J. Melosh, *ibid.* **98**, E5319 (1993).
18. See (*8*); C.-Y. Shih *et al.*, *Geochim. Cosmochim. Acta* **46**, 2323 (1982); J. H. Chen and G. J. Wasserburg, *Lunar Planet. Sci.* **XVI**, 113 (1986); *Geochim. Cosmochlm. Acta* **50**, 955 (1986). An overview of isotopic evidence for early differentiation is given by Jagoutz (*14*). Differences in the isotopic abundance of ^{129}Xe between the martian atmosphere and indigenous Xe in Chassigny are also consistent with early I/Xe fractionation on Mars when ^{129}I (half-life of 16 million years) was still live. See D. S. Musselwhite, M. J. Drake, and T. D. Swindle [*Nature* **352**, 697 (1991), and references therein].
19. J. J. Lissauer, *Icarus* **69**, 249 (1987).
20. D. J. Stevenson and J. I. Lunine, *ibid.* **75**, 146 (1988).
21. G. W. Wetherill and G. R. Stewart, *ibid.* **77**, 350 (1989); *ibid.* **106**, 190 (1993); D. Spaute, S. J. Weidenschilling, D. R Davis, F. Marzari, *ibid.* **92**, 147 (1991); S. J. Aarseth, D. N. C. Lin, P. L. Palmer, *Astrophys. J.* **403**, 351 (1993).
22. R. B. Larson, in *The Formation and Evolution of Planetary Systems*, H. A. Weaver and L. Danly, Eds. (Cambridge Univ. Press, New York, 1989), pp. 31–54; G. B. Wetherill, *Icarus* **100**, 307 (1992).
23. J. J. Lissauer, J. B. Pollack, G. W. Wetherill, D. J. Stevenson, in *Neptune and Triton*, D. P. Cruikshank and M. S. Matthews, Eds. (Univ. of Arizona Press, Tucson, in press).
24. G. W. Wetherill, in *Origin of the Moon*, W. K. Hartmann, R. J. Phillips, G. J. Taylor, Eds. (Lunar and Planetary Institute, Houston, 1986), pp. 519–550.
25. L. E. Nyquist *et al.*, *Geochim. Cosmochim. Acta* **54**, 2195 (1990).
26. L. E. Nyquist *et al.*, in preparation.
27. Small ^{142}Ce and ^{144}Sm interferences were monitored simultaneously by means of ^{140}Ce and ^{147}Sm and corrected on a ratio-by-ratio basis. We checked the validity of these corrections carefully for any correlation between $^{142}Nd/^{144}Nd$ and $^{142}Ce/^{142}Nd$ or $^{144}Sm/^{144}Nd$, using both sample run data and Ce-doped Nd standards. No evidence for systematic error from interferences was observed to within the run precision, even for ^{142}Ce corrections greatly in excess of those made in sample runs. Interference of $^{130}Ba^{16}O$ on ^{146}Nd was monitored by means of mass-154 ($^{138}Ba^{16}O$) but never observed. We controlled electronic drifts by determining gain factors on all channels four times during each run. A large number of standards (91) were run in order to quantify analytical precision and long-term drift in detector efficiency. Shifts in $^{142}Nd/^{144}Nd$ were determined relative to mean values of "local standards." The typical 2σ external precision ($2\sigma_p$) of ±29 ppm for a single measurement was determined from the observed variances of both multiply run samples and the standard. The greater estimate of sample variance was always chosen if the variance of sample multiplicates was greater than the variance on standards. The typical precision of the standard composition determined locally was ±10 ppm ($2\sigma_m$). The

typical quadratic sum of uncertainties in the sample and the local standards reference is ±20 ppm ($2\sigma_m$) for a triplicate sample analysis with the $^{146}Nd/^{144}Nd$ normalization. We estimated uncertainties in the mean determinations for samples and groups by weighting individual values inversely as the square of individual uncertainties. Our best estimate of the absolute value of $^{142}Nd/^{144}Nd$ ratio of the JSC Ames metal Nd standard is 1.138264 ± 28, normalized to $^{146}Nd/^{144}Nd$ = 0.724140 (*25*). A more detailed description of the method of data reduction and justification of error assignments is given in (*26*).
28. This work was supported by the National Aeronautics and Space Administration and a National Research Council postdoctoral research fellowship to C.L.H. Interest and encouragement from A. G. W. Cameron and S. B. Jacobsen are gratefully acknowledged.

17 March 1993; accepted 9 November 1994

Oscillating Stereocontrol: A Strategy for the Synthesis of Thermoplastic Elastomeric Polypropylene

Geoffrey W. Coates and Robert M. Waymouth*

A strategy has been developed for the synthesis of thermoplastic elastomeric polypropylene based on the catalytic activity of the unbridged metallocene bis(2-phenylindenyl)zirconium dichloride [$(2\text{-PhInd})_2ZrCl_2$]. This catalyst was designed to isomerize between achiral and chiral coordination geometries during the polymerization reaction to produce atactic-isotactic stereoblock polymers. The metallocene precursor $(2\text{-PhInd})_2ZrCl_2$ in the presence of methylaluminoxane polymerizes propylene to yield rubbery polypropylene. The isotacticity of the polymer, described by the isotactic pentad content, increases with increasing propylene pressure and decreasing polymerization temperature to produce polypropylenes with an isotactic pentad content ranging from 6.3 to 28.1 percent.

The stereochemistry of polyolefins strongly influences their properties. Isotactic polypropylene, consisting of a regular arrangement of stereocenters, is a crystalline thermoplastic with a melting point of ~165°C, whereas atactic (stereorandom) polypropylene is an amorphous gum elastomer. Polypropylene consisting of blocks of atactic and isotactic stereosequences is a rubbery material with properties of a thermoplastic elastomer (*1*) (Fig. 1). Natta was the first to produce rubbery polypropylene and to interpret the elastomeric properties of this material in terms of a stereoblock structure consisting of blocks of crystallizable isotactic stereosequences and amorphous atactic stereosequences (*2*). Collette and co-workers subsequently reported improved catalysts for the synthesis of polypropylene with elastomeric properties based on the use of Zr and Ti alkyls on alumina supports (*3*), and Chien and coworkers reported the synthesis of elastomeric polypropylene using a stereorigid titanocene catalyst (*4*). Chien *et al.* proposed that polymerization occurs alternately at aspecific and isospecific coordination sites to give a stereoblock structure. Although these catalyst systems represent significant advances for the synthesis of elastomeric polypropylene, it has so far proven difficult to control the polymer structure and properties through a rational modification of the catalysts or reaction conditions.

In this report, we introduce a strategy for dynamic stereocontrol in the polymerization of α-olefins. We describe an olefin polymerization catalyst that was designed to isomerize between achiral and chiral coordination geometries in order to produce atactic-isotactic stereoblock poly(α-olefins). This strategy provides a means of controlling the distribution of isotactic and atactic stereosequences to produce polymers that exhibit a wide range of elastomeric properties depending on the reaction conditions.

The advent of homogeneous stereospecific olefin polymerization catalysts has ushered in a new era in olefin polymerization. As described in the pioneering studies of Brintzinger and co-workers (*5*), Ewen (*6*), and Kaminsky *et al.* (*7*), chiral racemic *ansa*-metallocenes produce isotactic polyolefins, whereas achiral meso isomers form atactic polyolefins (Fig. 2) (*6*, *7*). To produce stereoblock polymers, we prepared an unbridged metallocene catalyst that was designed to isomerize between chiral *rac*-like and achiral *meso*-like geometries by rotation of the indenyl ligands about the metal-ligand bond axis (*8*). A phenyl substituent on the indene ligand was chosen to inhibit the rate of ligand rotation such that it would be slower than that of monomer insertion yet faster than the time required to construct one polymer chain in order to produce atactic-isotactic stereoblock copolymers (Fig. 3) (*9*). These catalysts can thus oscillate between aspecific and isospecific coordination geometries.

The metallocene bis(2-phenylindenyl)-zirconium dichloride, $(2\text{-PhInd})_2ZrCl_2$, was isolated in 82% yield from the reaction of 2-phenylindenyllithium and $ZrCl_4$ (*10*). Analysis of the complex by ^1H nuclear magnetic resonance (NMR) spectroscopy between 25° and −100°C was consistent with molecular C_{2v} symmetry, as commonly observed for metallocenes in rapid

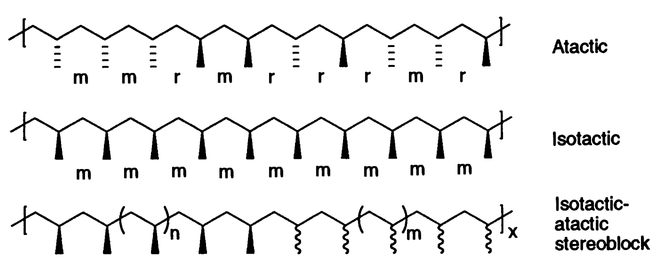

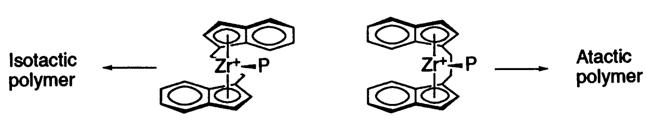

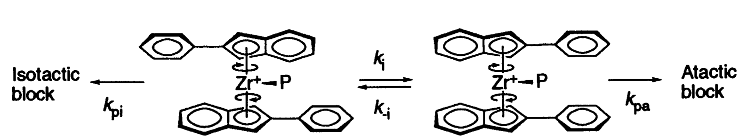

Fig. 1 (top). Isotactic, atactic, and stereoblock polypropylene (*17*). **Fig. 2 (middle).** Stereorigid *ansa*-metallocenes for the production of isotactic and atactic polymers. **Fig. 3 (bottom).** Oscillating catalyst for the production of stereoblock polymers.

Department of Chemistry, Stanford University, Stanford, CA 94305, USA.

*To whom correspondence should be addressed.